Electronic Supplementary Material (ESI) for Polymer Chemistry.

SUPPORTING INFORMATION

Synthesis and supramolecular organization of chiral poly(thiophene)-magnetite hybrid nanoparticles

*Ward Ceunen[1], Annelien Van Oosten[1], Rick Vleugels[2], Julien De Winter[3], Pascal Gerbaux[3], Zhi Li[4], Steven de Feyter[4], Thierry Verbiest[2] and Guy Koeckelberghs[1]**

[1]Laboratory for Polymer Synthesis, Department of Chemistry, KU Leuven, Celestijnenlaan 200F, B-3001 Heverlee, BELGIUM

[2]Molecular Imaging and Photonics, Department of Chemistry, KU Leuven, Celestijnenlaan 200F, B-3001 Heverlee, BELGIUM 200D, 3001 Leuven, BELGIUM

[3]Organic Synthesis and Mass Spectrometry Laboratory, Interdisciplinary Center for Mass Spectrometry, University of Mons-UMONS, 23 Place du Parc, 7000 Mons, BELGIUM

[4]Division of Molecular Imaging and Photonics, Department of Chemistry, KU Leuven, Celestijnenlaan 200F, B-3001 Heverlee, BELGIUM

I. TABLE OF CONTENTS

II. MATERIALS

All reagents were purchased and used without further purification. Reagent grade solvents were dried over columns with activated alumina by a MBRAUN SPS 800 system.

III. INSTRUMENTATION

^{1}H-NMR spectra were recorded on a Bruker Avance 300 MHz, Bruker Avance 400 MHz or Bruker Avance 600 MHz spectrometer.

Gel permeation chromatography (GPC) measurements were carried out on a Shimadzu 10A GPC system. The column is a PLgel 5μm mixed-D type column and the detection system consists of a differential refractometer and a UV-vis spectrophotometer. The GPC system is calibrated towards polystyrene standards (purchased from Polymer Laboratories). Before measuring, the polymers are dissolved in THF ($c \approx 1$ mg/mL) and filtered over a pore size of 0.2 μm.

UV-vis spectra were recorded with a Perkin Elmer Lambda 900UV-vis NIR spectrometer.

CD spectra were obtained with a JASCO J-810 spectrometer.

Matrix-assisted laser desorption/ionization time-of-flight (MALDI-ToF) mass spectra were recorded using a Waters QToF Premier mass spectrometer equipped with a Nd-YAG laser of 355 nm with a maximum pulse energy of 65μJ delivered to the sample at 50 Hz repeating rate. Time-of-flight mass analyses were performed in the reflection mode at a resolution of about 10 000. The matrix, trans-2-(3-(4-tert-butyl-phenyl)-2-methyl-2-propenylidene)malononitrile (DCTB), was prepared as a 40 mg/mL solution in chloroform. The matrix solution (1 μL) was applied to a stainless steel target and air-dried. Polymer samples were dissolved in chloroform to obtain 1

mg/mL solutions. Then, 1 μL aliquots of these solutions were applied onto the target area (already bearing the matric crystals) and then air-dried.

AFM measurements were carried out in air using a Multimode AFM with a Nanoscope VIII controller (Veeco/Digital Instruments) in intermittent contact mode. Olympus silicon cantilevers (OMCL-AC160TS; drive frequency 200–400 kHz) were used. AFM images were processed using WSxM (Nanotec Electronica, Spain).[1]

Transmission electron microscopy measurements were performed on a 80 kV Zeiss EM-900 using Ted Pella 300 mesh Formvar carbon coated copper grid. Distribution data were calculated by ImageJ. Oleic acid-coated nanoparticles were dispersed in heptane and deposited onto the grid, while the hybrid materials were dispersed in THF before deposition.

Thermogravimetric analyses (TGA) were performed on a Q500 V20.13 equipment with a standard furnace (TAInstruments, Brussels, Belgium). The weight losses of 10 mg samples in aluminum pans were monitored as they were heated from room temperature to 823 K at 10 K/min under N_2 (40 mL/min).

The Faraday setup consists of a broad wavelength laser driven light source, followed by a monochromator to scan different wavelengths. The light then travels through a polarizer, a PEM, the sample which is mounted in a DC magnet and an analyzer to finally hit a photomultiplier tube (PMT). If the analyzer is set to a correct angle, 45° in comparison to the first polarizer, and the correct detection frequency is used (the double frequency of the operating frequency of the PEM in our case), the resulted intensities recorded by the PMT can be related to CB in the sample.[2] By measuring the CB in the sample for a set of discrete magnetic field strengths and fitting this to the resulting magnetic induction, one can obtain the Verdet constant.

Concerning the calculation of the contributions of the magnetite nanoparticle and the polymer in the hybrid material

For Faraday rotation, the angle of rotation Θ is given by: Θ=VBL where B is the magnetic field in the propagation direction, L the path length of the light in the sample and V the Verdet constant, a material property that quantifies Faraday rotation. The magnetic flux density, B can be decomposed in the applied magnetic field H and the magnetization of the material, M. As such we can write: Θ=V(H+M)L. The magnetization, M, is caused by a diamagnetic term linear in magnetic field from organic substances and a superparamagnetic term from the nanoparticles. The magnetization response of these samples is best described by a Langevin function. For the fitting of the Faraday rotation, the following equation was used:

$$\Theta=A+B*((\cosh(C*H)/\sinh(C*H))-(1/(C*H)))+D*H$$

Here, A represents an offset factor, B is directly proportional to Faraday rotation, C is a parameter within the Langevin function which determines the shape of the curve and D represents the linear diamagnetic response. This way, the contributions of diamagnetic materials and superparamagnetic materials to the Faraday rotation can be determined.

IV. SYNTHETIC PROCEDURES

The monomers[3] and initiators[4] were synthesized according to literature procedures.

a. Synthesis of the initiator

4-bromo-5-methyl-1,2-benzenediol

Br_2 (16.11 mmol; 2.57 g) is added dropwise to a solution of 4-methyl-1,2-benzenediol (16.11 mmol; 2.00 g) in DCM (100 mL) under Ar. The flask is sealed with a $CaCl_2$-tube and the mixture

is stirred overnight at room temperature. The mixture is washed with a saturated $NaHSO_4$-solution and the product extracted with DCM. After removal of the solvent under reduced pressure, the product was purified via recrystallization in DCM. The pure product was obtained as white crystals.

Yield = 2.17 g (67 %)

^{1}H NMR (300 MHz, $CDCl_3$): δ = 7.05 (s, 1 H); 6.76 (s, 1 H); 5.11 (s, 2 H); 2.27 (s, 3 H)

1-bromo-4,5-bis[[(1,1-dimethylethyl)dimethylsilyl]oxy]-2-methylbenzene

To a solution of 4-bromo-5-methyl-1,2-benzenediol (10.70 mmol; 2.17 g) and imidazole (32.05 mmol; 2.18 g) in dry THF (40 mL) under Ar, *tert*-Bbutyldimethylsilyl chloride (32.05 mmol; 4.83 g) in dry THF (40mL) is added. The mixture is stirred overnight at room temperature. The mixture is subsequently washed with $NaOH_{(aq)}$ (0.1 M) and $HCl_{(aq)}$ (0.1 M) and the product extracted with Et_2O. The organic layer was washed with a saturated $NaHCO_3$-solution and dried over $MgSO_4$.The solvent was removed under reduced pressure and the product purified using column chromatography (SiO_2, eluent: heptane/ethyl acetate 85/15). The pure product was obtained as white crystals.

Yield = 3.74 g (81 %)

^{1}H NMR (300 MHz, $CDCl_3$): δ = 6.97 (s, 1 H); 6.69 (s, 1 H); 2.25 (s, 3 H); 0.97 (s, 18 H); 0.19 (s, 6 H); 0.18 (s, 6 H)

4-bromo-5-methyl-1,2-diacetate-1,2-benzenediol

A solution of 4-bromo-5-methyl-1,2-benzenediol (14.40 mmol; 2.9 g) in acetic anhydride (100 mL), under Ar and shielded from light, is stirred overnight at room temperature. The product is

extracted with DCM. The solvent was removed under reduced pressure and the product purified via recrystallization in EtOH. The pure product was obtained as white crystals.

Yield = 1.71 g (41 %)

^{1}H NMR (300 MHz, $CDCl_3$): δ = 7.38 (s, 1 H); 7.07 (s, 1 H); 2.37 (s, 3 H); 2.28 (s, 6 H)

$Ni(PPh_3)_4$

$Ni(PPh_3)_4$ was synthesized according to literature procedures.[5]

cat.$(PPh_3)_2$ *and* ***o-tol.$(PPh_3)_2$*** *precursor initiators*

The **cat.$(PPh_3)_2$** and ***o*-tol.$(PPh_3)_2$** precursor initiators and were synthesized according to literature procedures by insertion of $Ni(PPh_3)_4$ into the corresponding functionalized aryl bromide in dry toluene under Ar.[3] After concentration of the reaction mixture under reduced pressure, the product is obtained as a yellow solid upon precipitation in pentane and subsequent filtration over a glass filter.

Yield ***o*-tol.$(PPh_3)_2$** = 0.120 g (85 %)

^{1}H NMR (300 MHz, $CDCl_3$): δ = 7.52 (m, 12 H); 7.32 (m, 6 H); 7.23 (m, 12 H); 7.09 (d, 1 H); 6.26 (m, 2 H); 5.91 (d, 1 H); 2.10 (s, 3 H)

^{31}P NMR (162 MHz $CDCl_3$, calibrated toward H_3PO_4 85%): 23.9 ppm

Yield **cat.$(PPh_3)_2$** = 0.243 g (55 %)

^{1}H NMR (300 MHz, $CDCl_3$): δ = 7.57 (s, 12 H); 7.33 (m, 6 H); 7.27 (m, 12 H); 6.84 (s, 1 H); 5.71 (s, 1 H); 2.13 (s, 3 H); 2.07 (s, 3 H); 2.00 (s, 3 H)

^{31}P NMR (162 MHz $CDCl_3$, calibrated toward H_3PO_4 85%): 21.48

Prior to the polymerization these precursor initiators **cat.(PPh$_3$)$_2$** and ***o*-tol.(PPh$_3$)$_2$** undergo a ligand exchange with eq. of 1,3-bis(diphenylphosphino)propane (dppp) in dry THF to form the **cat.** and ***o*-tol.** initiators respectively.

b. Synthesis of the monomer

(+)-(*S*)-2-bromo-5-iodo-3-(3,7-dimethyloctyl)thiophene was prepared according to literature procedures.[4] 2-bromo-5-iodo-3-(3,7-dimethyloctyl)thiophene is was bought from TCI and used without further purification.

c. Polymer synthesis

The polymers were synthesized according to literature procedures.[4] In a typical polymerization experiment, THF-solutions of initiator are stirred in several glass tubes for 20 minutes, together with 2 eq. of dppp. Parallel with this ligand exchange, the precursor monomer undergoes a Grignard metathesis (GRIM) reaction for 30 minutes in THF, induced by the addition of 1 eq. of *i*-propylmagnesium chloride. To initiate the polymerization, different volumes of this monomer solution are cannulated to the initiator solutions. After 60 minutes, the polymerization is terminated by adding HCl in THF.

d. Synthesis of the hybrid materials

The functionalization of the magnetite nanoparticles is a two-step one-pot reaction. For removal of the acetyl groups of the catechol functionality of the polymer, 0.1 mL of a 1 M NH_4OH solution in MeOH is added to a **cat.-P3DMOT** (35 mg) and Fe_3O_4-nanoparticle (1.5 mL mg) solution in THF (50 mg/mL) and stirred for 2h at room temperature. Subsequently, the activate catechol group of polymer couple to the nanoparticles, replacing the present oleic acid. The

hybrid material is purified via several series of solvation in THF, precipitation in MeOH and centrifugation.

V. Characterization of the polymers

a. GPC

o-tol.-P3DMOT

$[M]_0/[In]$	$\overline{M_n}$ [kg/mol]	Đ
20	4.7	1.1
40	9.3	1.1
60	14.6	1.1
80	20.3	1.1
100	20.1	1.2
120	21.5	1.2
140	23.6	1.2
160	21.5	1.2

cat.-P3HT

$[M]_0/[In]$	$\overline{M_n}$ [kg/mol]	Đ
20	4.4	1.2
40	8.5	1.1
60	12.2	1.1
80	16.9	1.1
100	15.1	1.1
120	24.7	1.1
140	27.3	1.2

cat.-P3DMOT

$[M]_0/[In]$	$\overline{M_n}$ [kg/mol]	Đ
20	3.0	1.2
40	7.0	1.1
60	10.2	1.1
80	14.2	1.2
100	15.0	1.2
120	15.5	1.2
140	12.9	1.2

b. NMR (400 MHz, $CDCl_3$)

o-tol.-P3DMOT

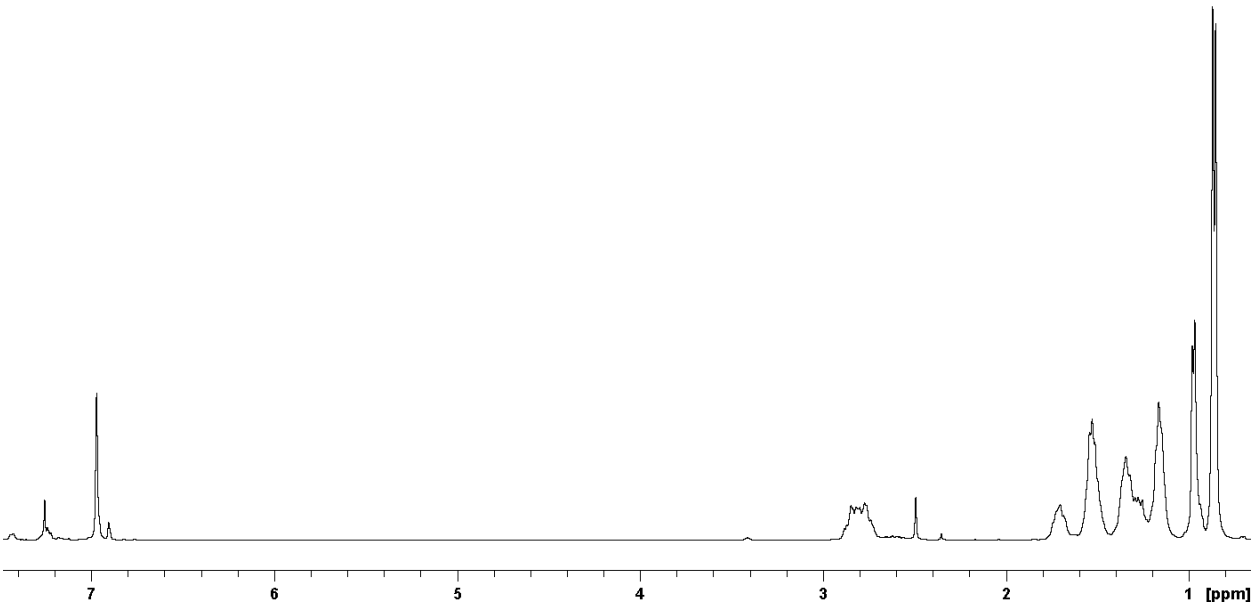

Figure S1. ^{1}H NMR spectrum of ***o*-tol.-P3DMOT** (M_n of 4.7 kg/mol).

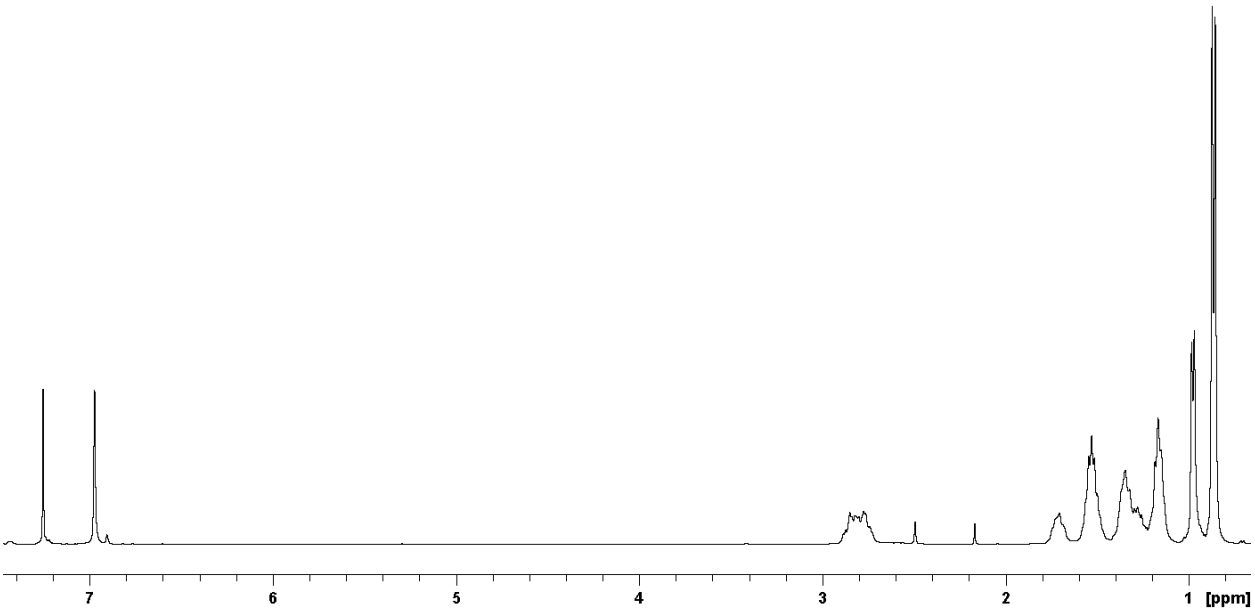

Figure S2. ^{1}H NMR spectrum of ***o*-tol.-P3DMOT** (M_n of 9.3 kg/mol).

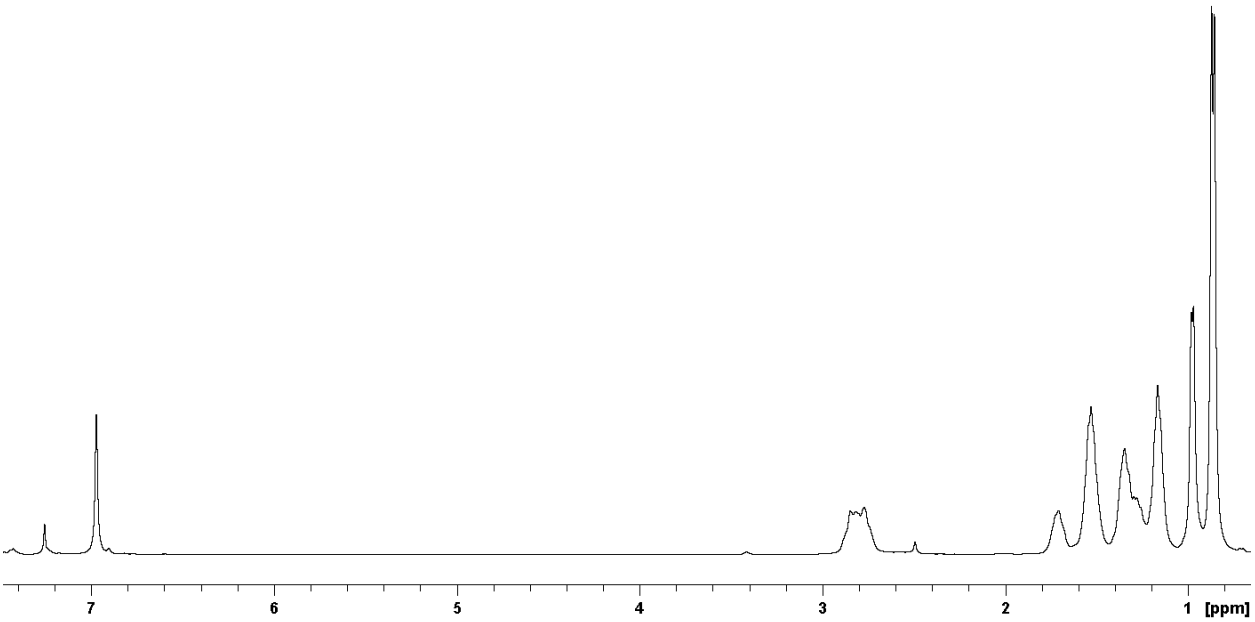

Figure S3. ^{1}H NMR spectrum of ***o*-tol.-P3DMOT** (M_n of 14.6 kg/mol).

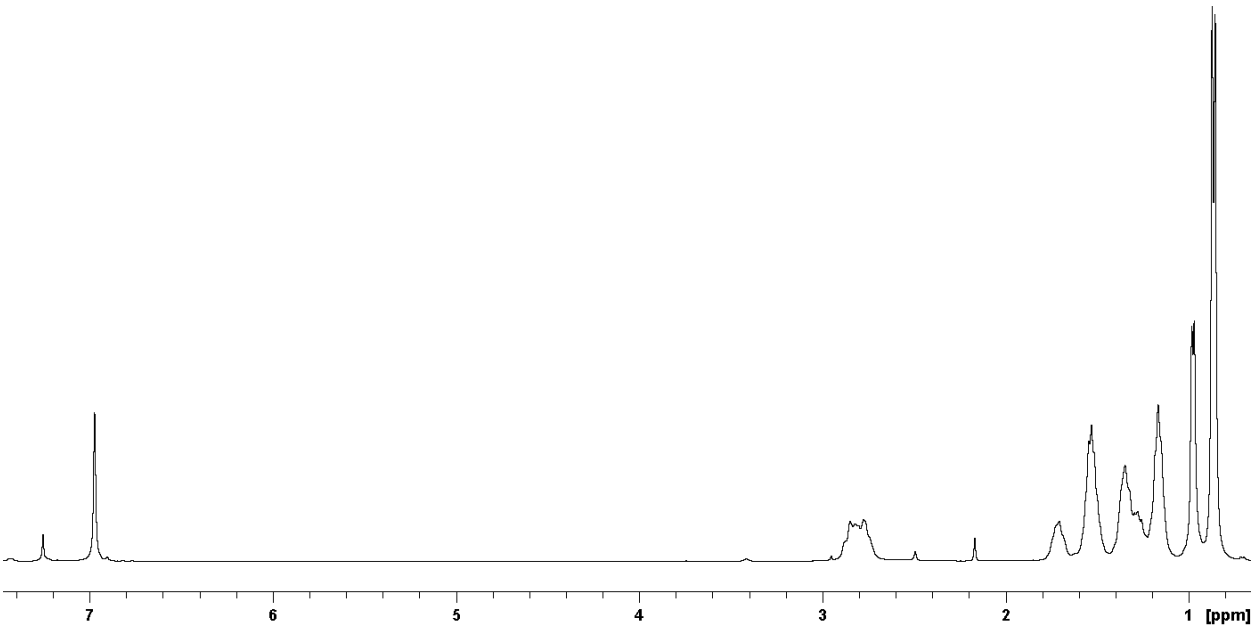

Figure S4. ^{1}H NMR spectrum of ***o*-tol.-P3DMOT** (M_n of 20.3 kg/mol).

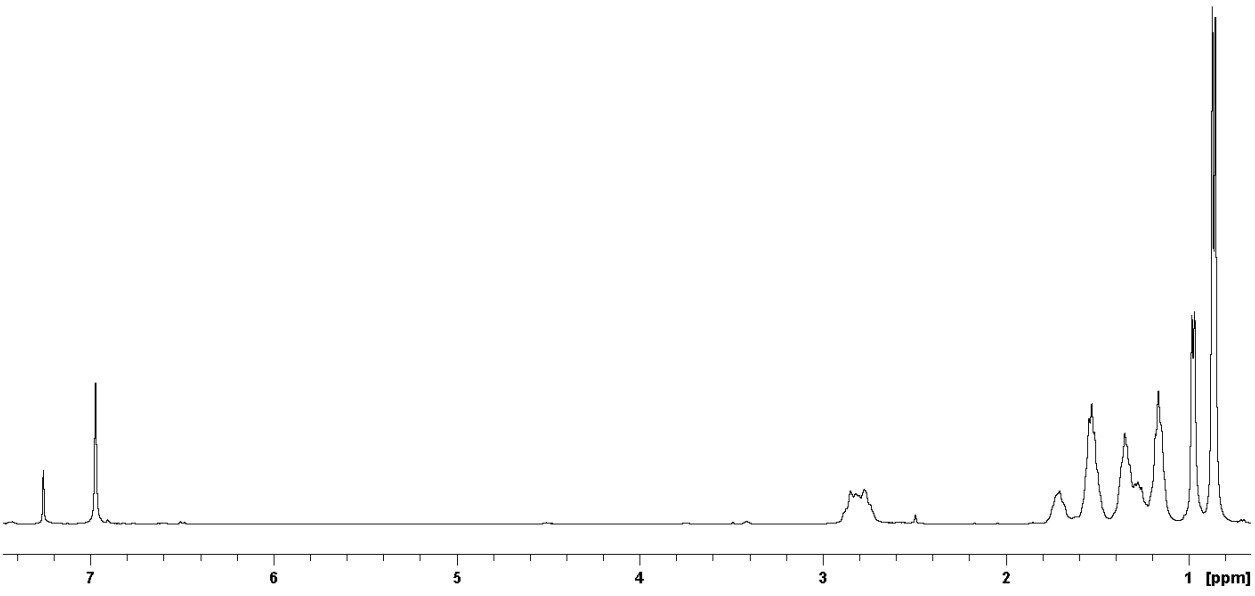

Figure S5. ^{1}H NMR spectrum of ***o*-tol.-P3DMOT** (M_n of 20.1 kg/mol).

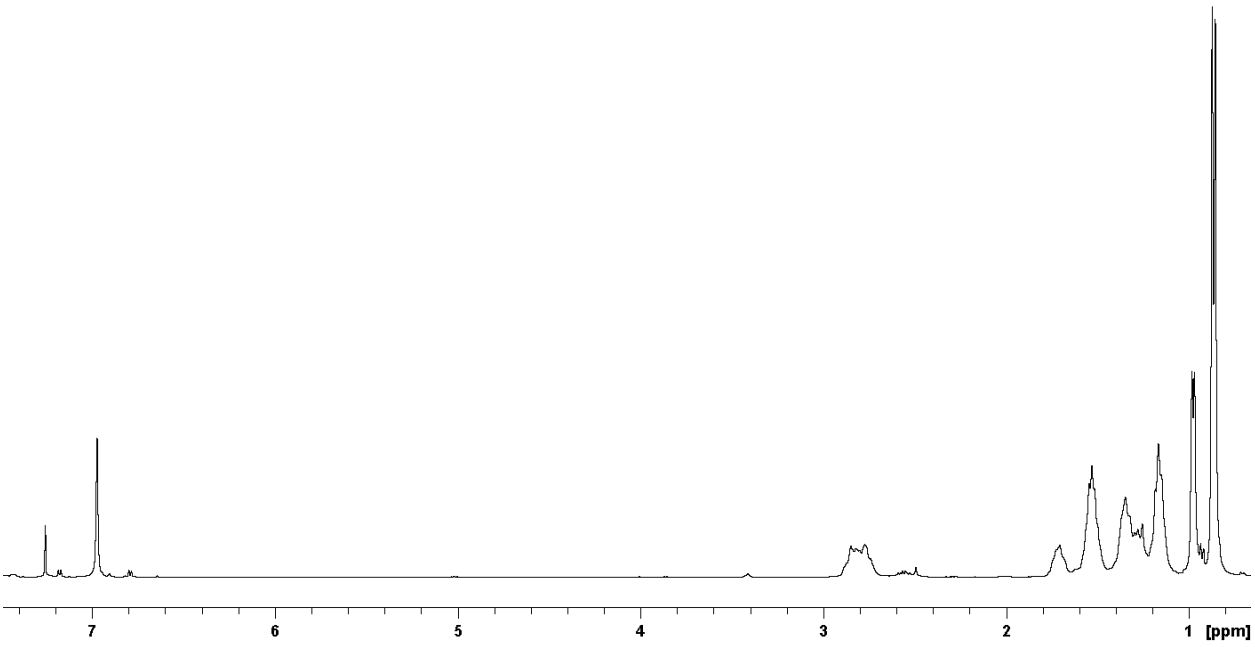

Figure S6. ^{1}H NMR spectrum of ***o*-tol.-P3DMOT** (M_n of 21.5 kg/mol).

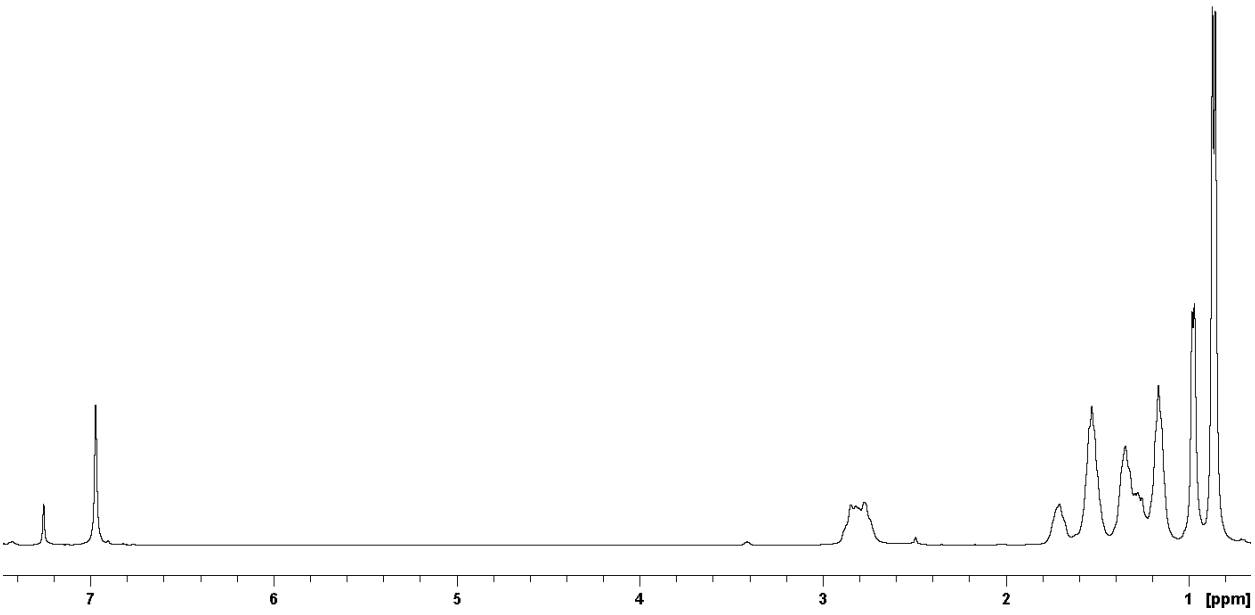

Figure S7. ^{1}H NMR spectrum of ***o*-tol.-P3DMOT** (M_n of 23.6 kg/mol).

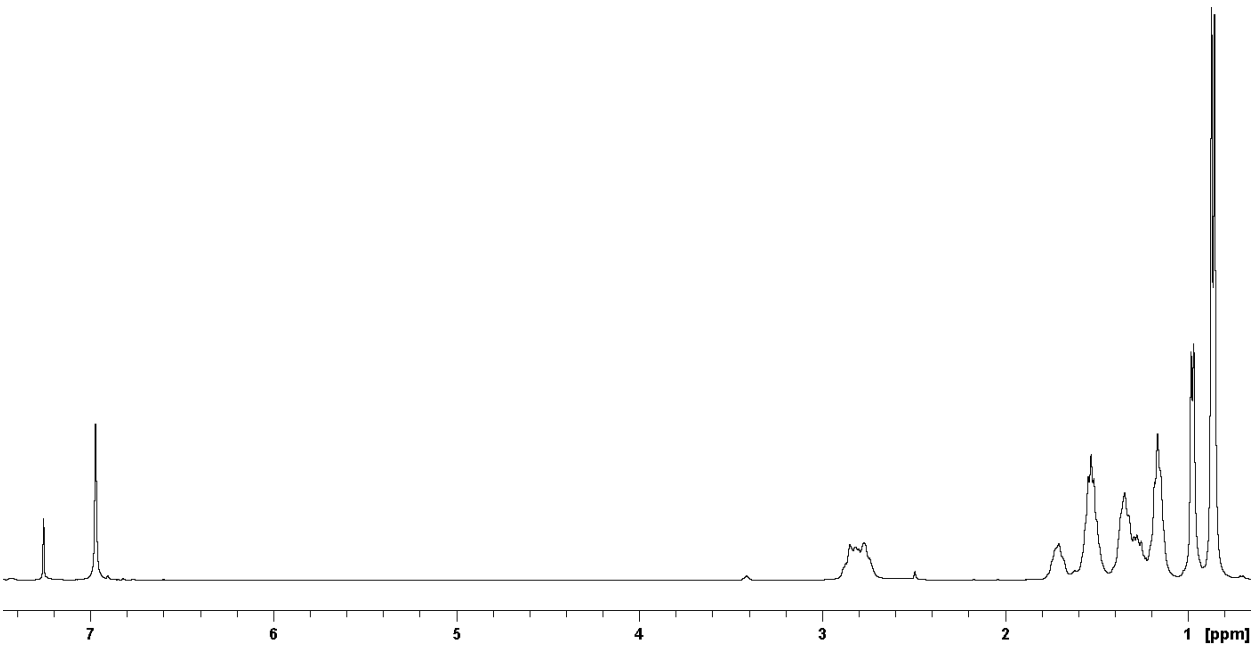

Figure S8. ^{1}H NMR spectrum of ***o*-tol.-P3DMOT** (M_n of 21.5 kg/mol).

cat.-P3HT

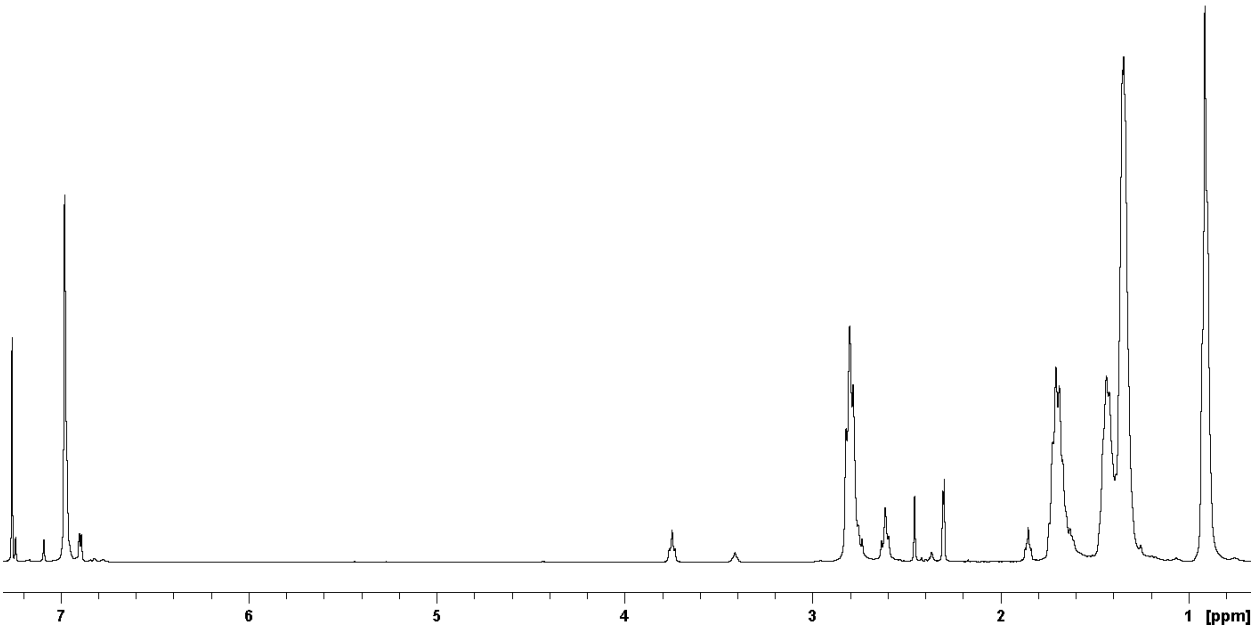

Figure S9. ^{1}H NMR spectrum of **cat.-P3HT** (M_n of 4.4 kg/mol).

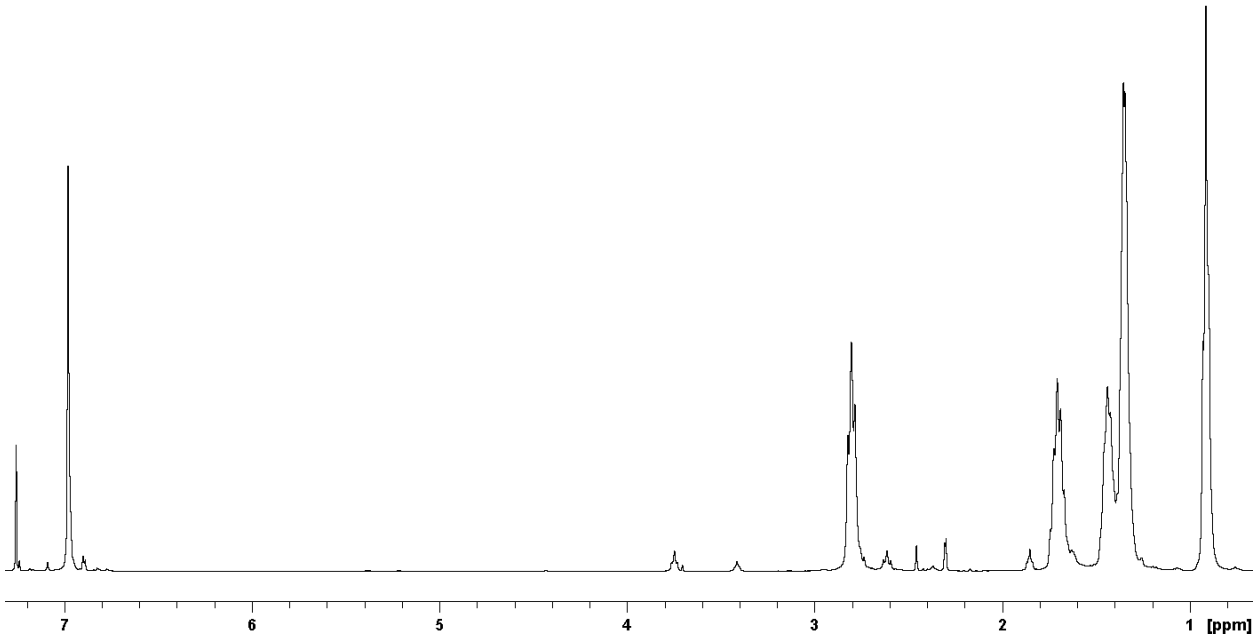

Figure S10. ^{1}H NMR spectrum of **cat.-P3HT** (M_n of 8.8 kg/mol).

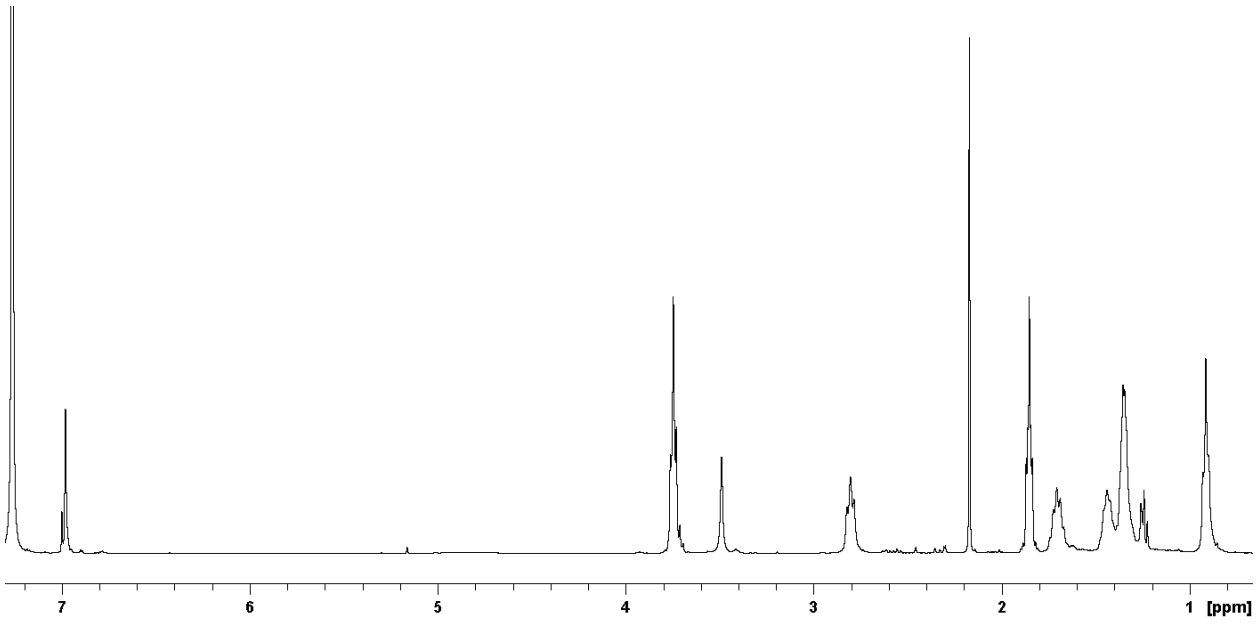

Figure S11. ^{1}H NMR spectrum of **cat.-P3HT** (M_n of 12.2 kg/mol).

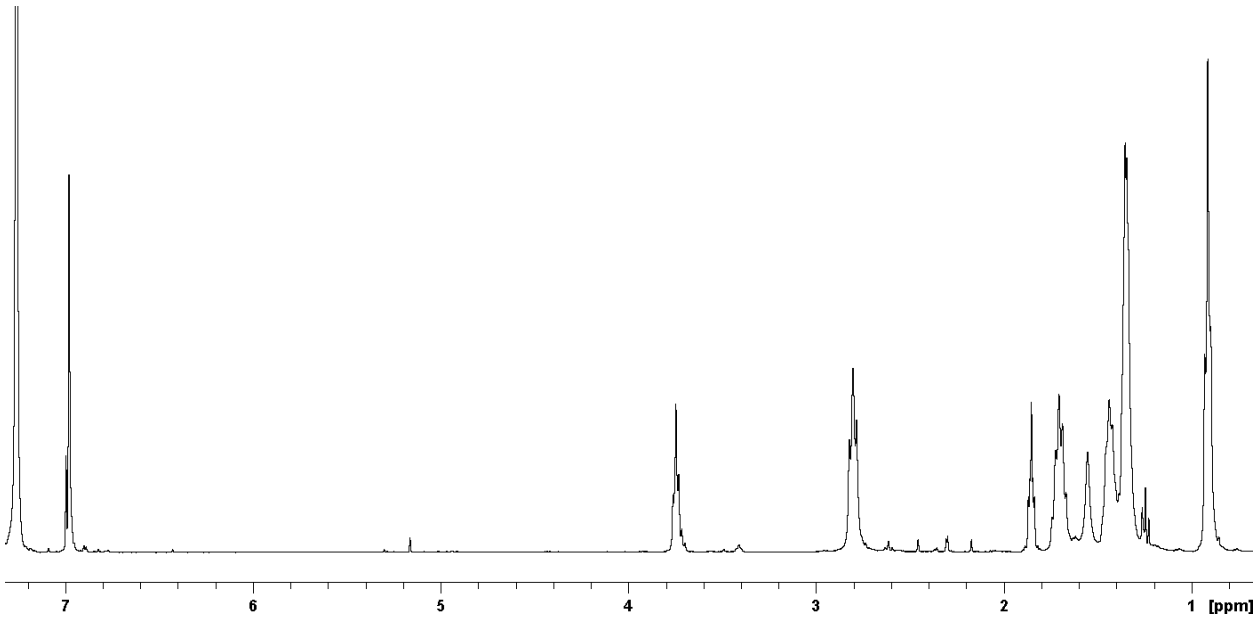

Figure S12. ^{1}H NMR spectrum of **cat.-P3HT** (M_n of 16.9 kg/mol).

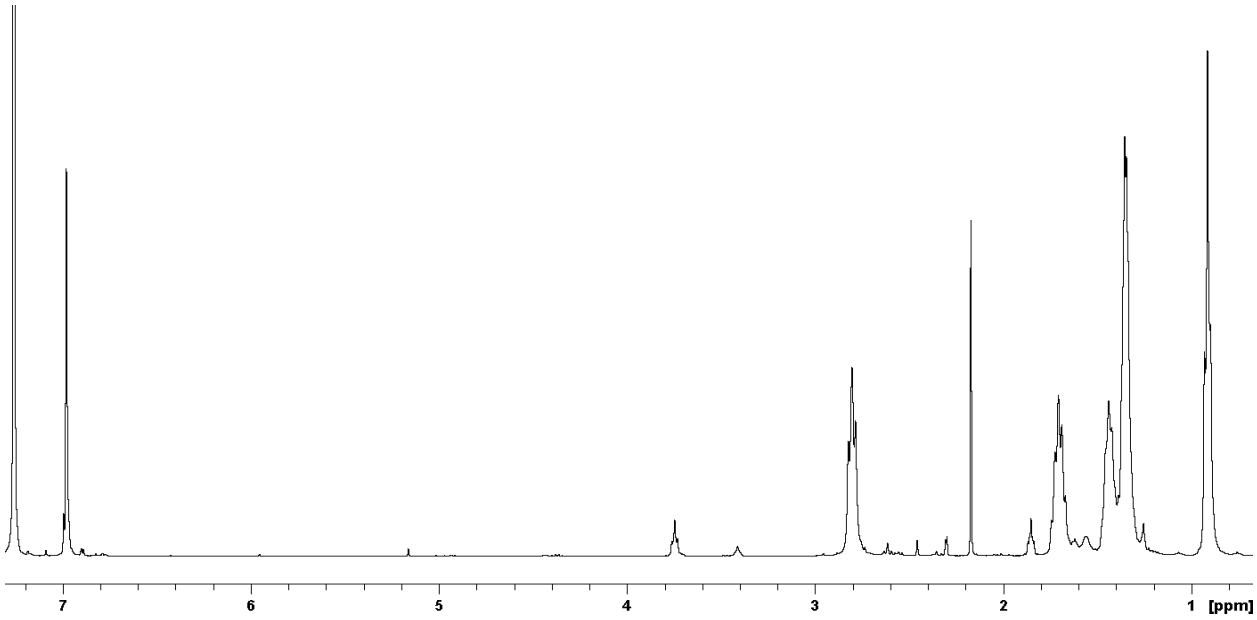

Figure S13. ^{1}H NMR spectrum of **cat.-P3HT** (M_n of 15.1 kg/mol).

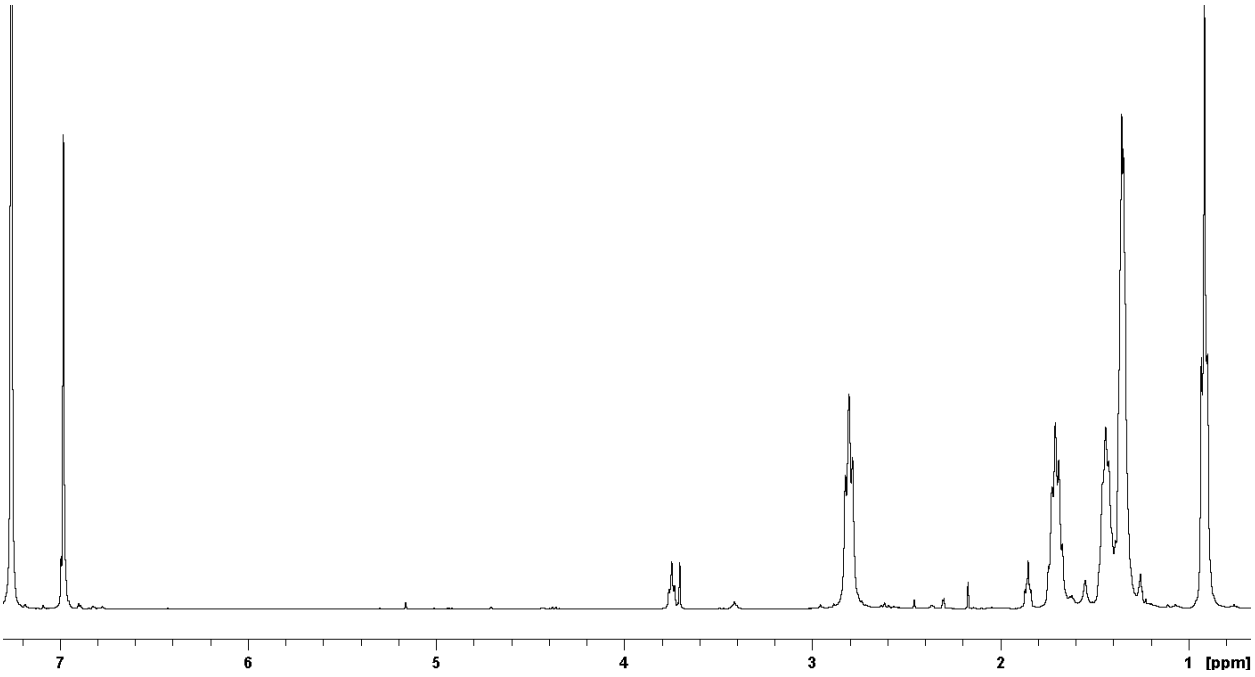

Figure S14. ^{1}H NMR spectrum of **cat.-P3HT** (M_n of 24.7 kg/mol).

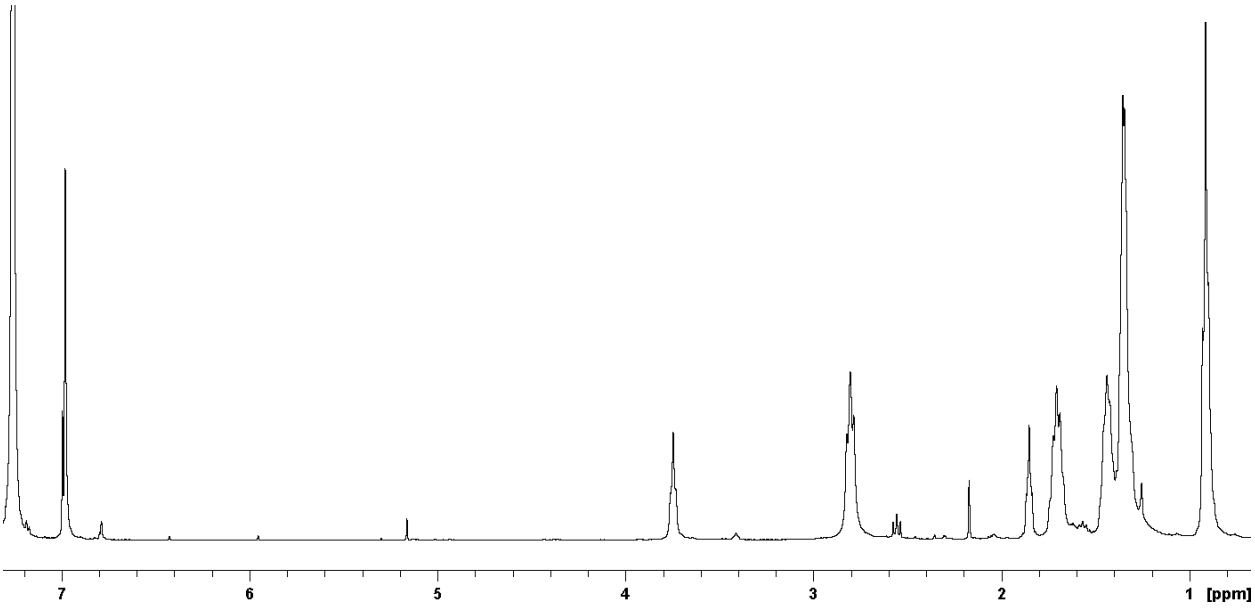

Figure S15. ^{1}H NMR spectrum of **cat.-P3HT** (M_n of 27.3 kg/mol).

cat.-P3DMOT

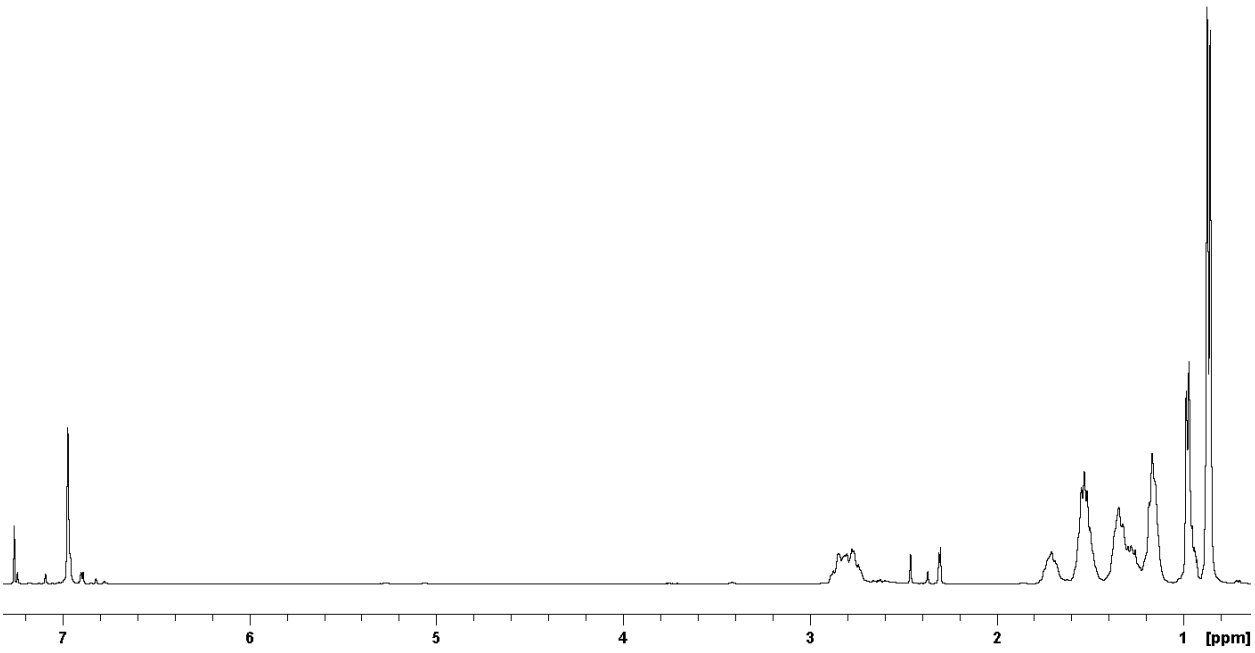

Figure S16. ^{1}H NMR spectrum of **cat.-P3DMOT** (M_n of 3.0 kg/mol).

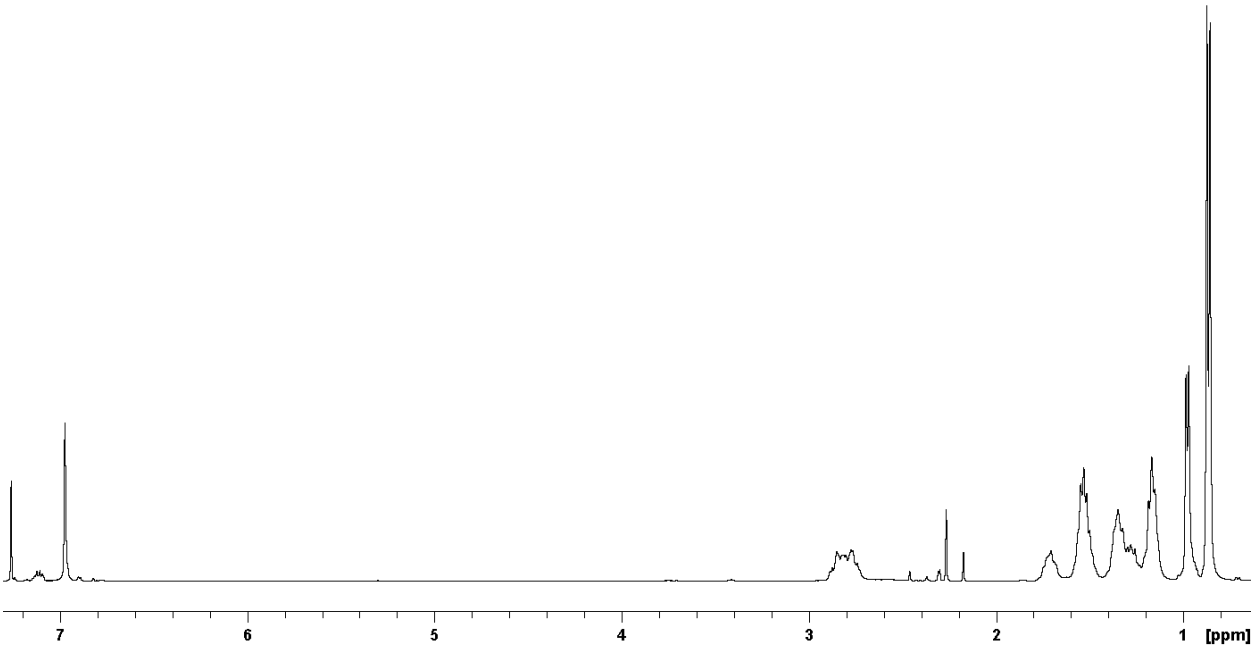

Figure S17. ^{1}H NMR spectrum of **cat.-P3DMOT** (M_n of 7.0 kg/mol).

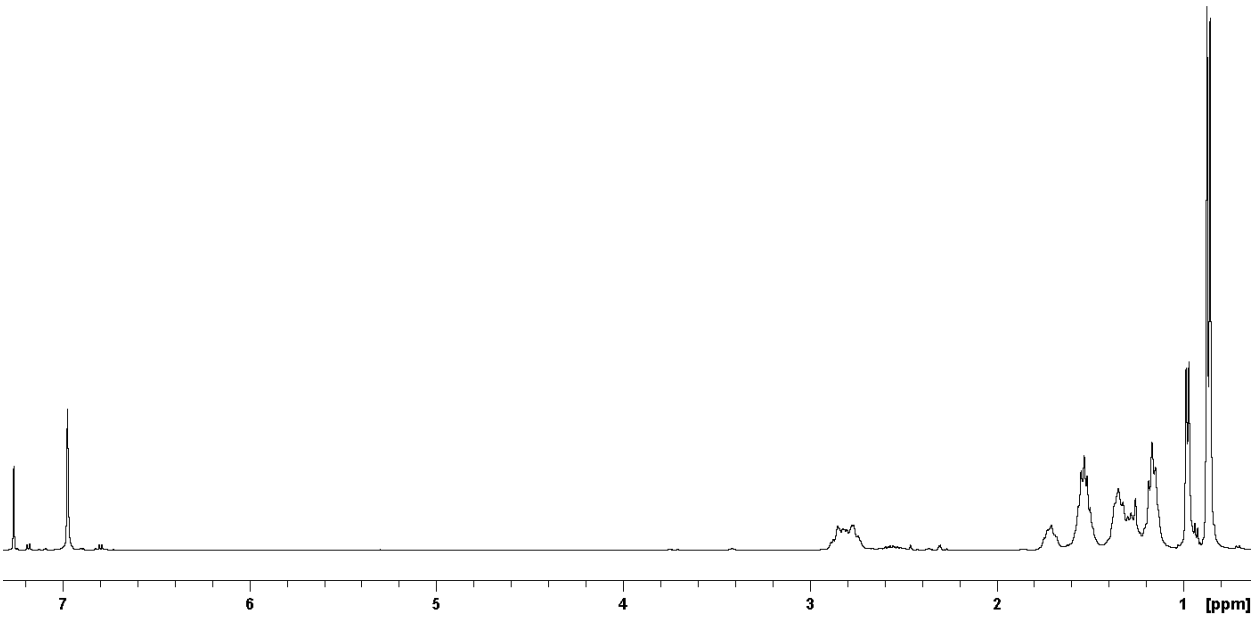

Figure S18. ^{1}H NMR spectrum of **cat.-P3DMOT** (M_n of 10.2 kg/mol).

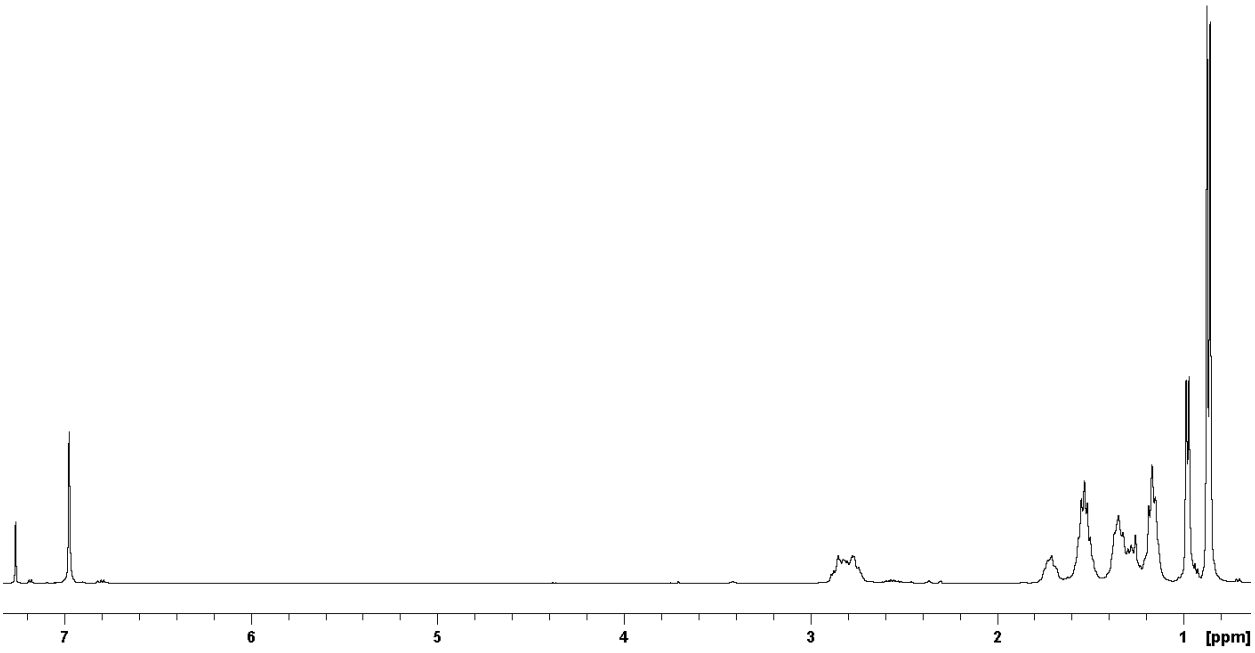

Figure S19. ^{1}H NMR spectrum of **cat.-P3DMOT** (M_n of 14.2 kg/mol).

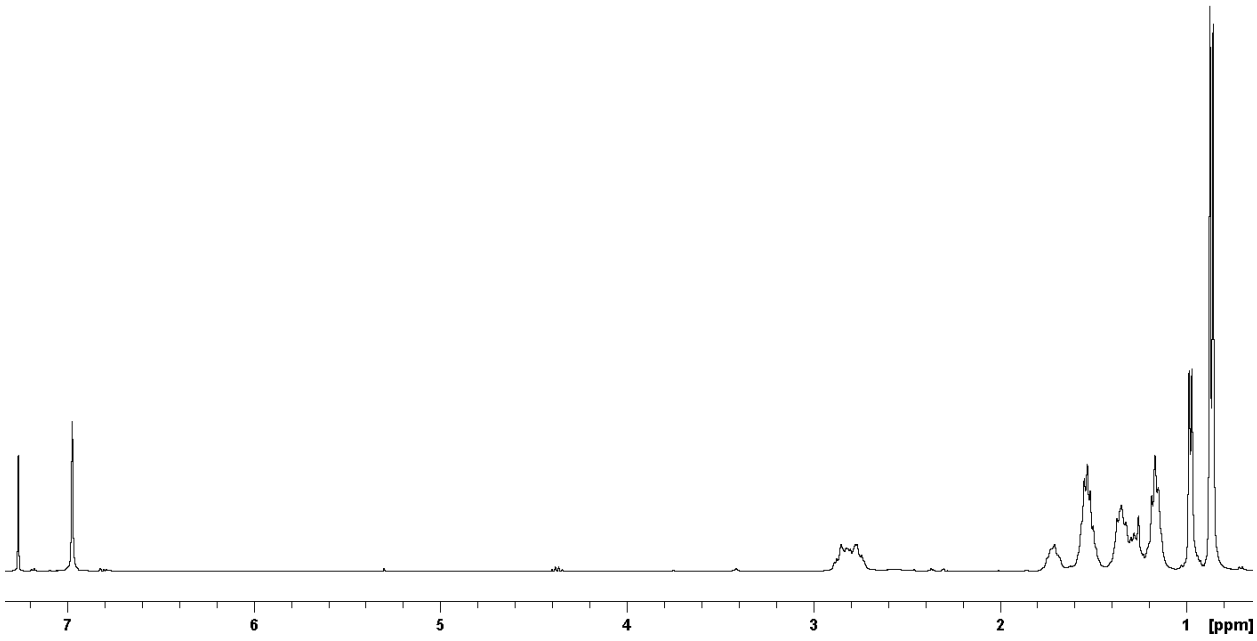

Figure S20. ^{1}H NMR spectrum of **cat.-P3DMOT** (M_n of 15.0 kg/mol).

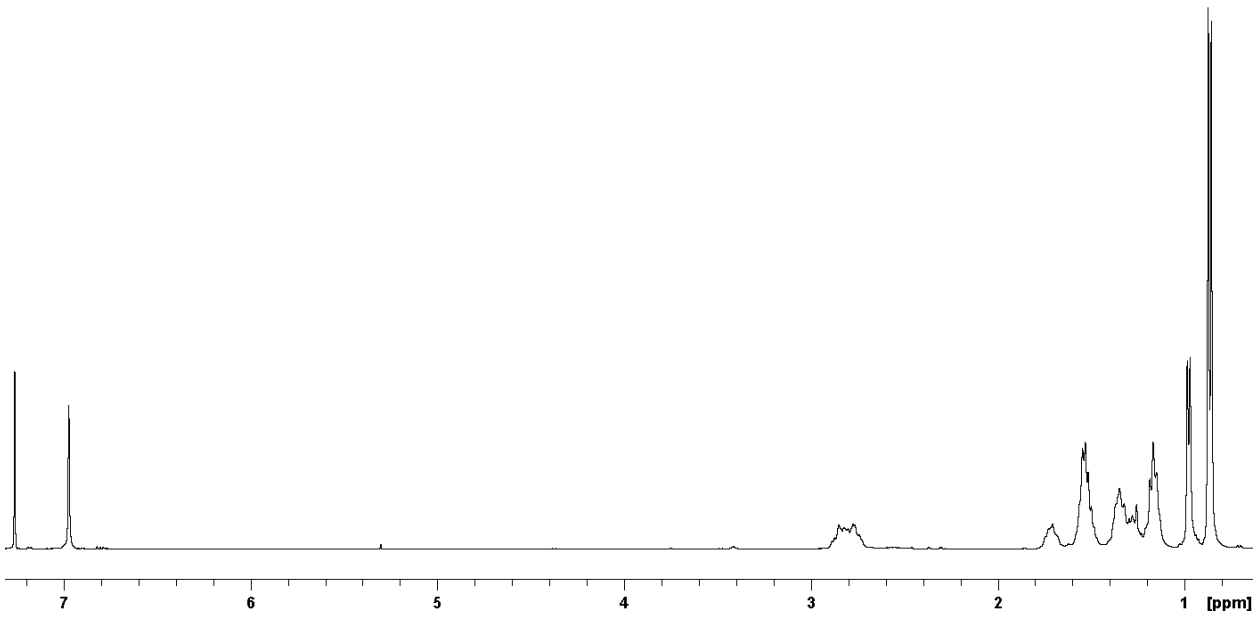

Figure S21. ^{1}H NMR spectrum of **cat.-P3DMOT** (M_n of 15.5 kg/mol).

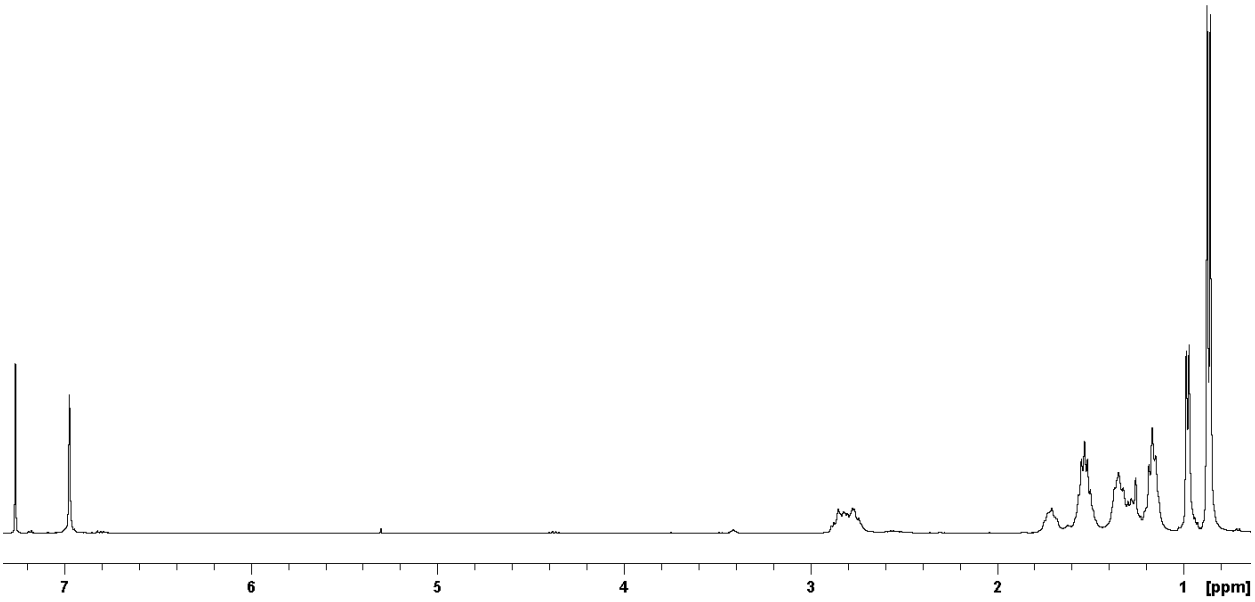

Figure S22. ^{1}H NMR spectrum of **cat.-P3DMOT** (M_n of 12.9 kg/mol).

c. MALDI-ToF

We note that, while GPC tends to overestimate the M_n of rod-like polymer chains, MALDI-ToF tends to ionize shorter chains more easily. This causes an increasing discrepancy between GPC and MALDI-ToF results for longer polymer chains.

cat.-P3HT

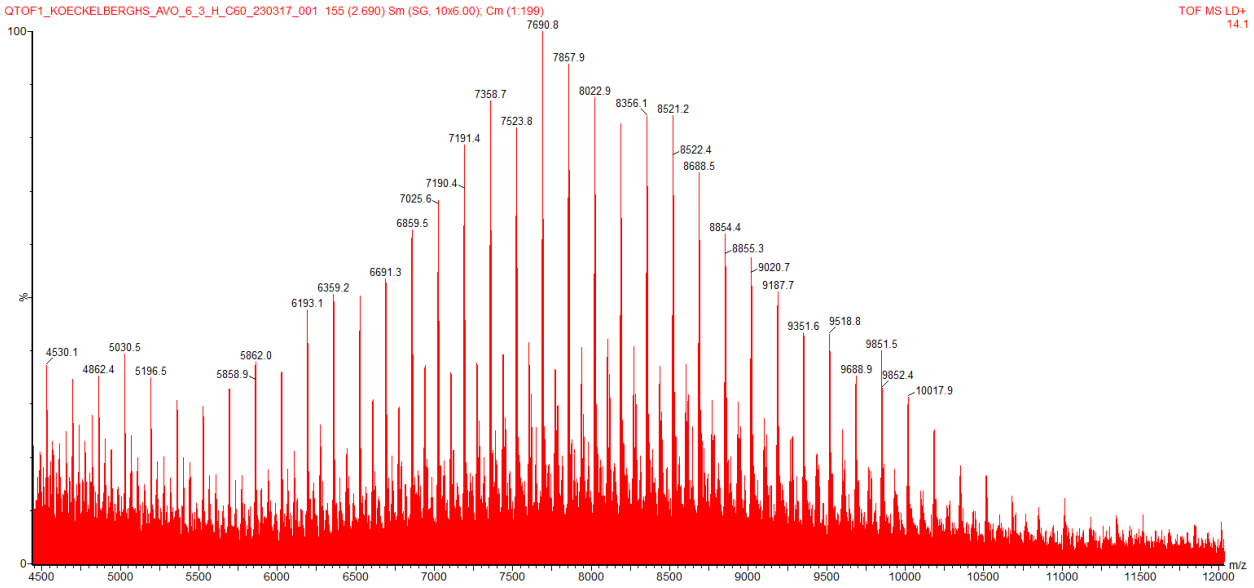

Figure S23. MALDI-ToF spectrum of **cat.-P3HT** (M_n of 12.2 kg/mol).

cat.-P3DMOT

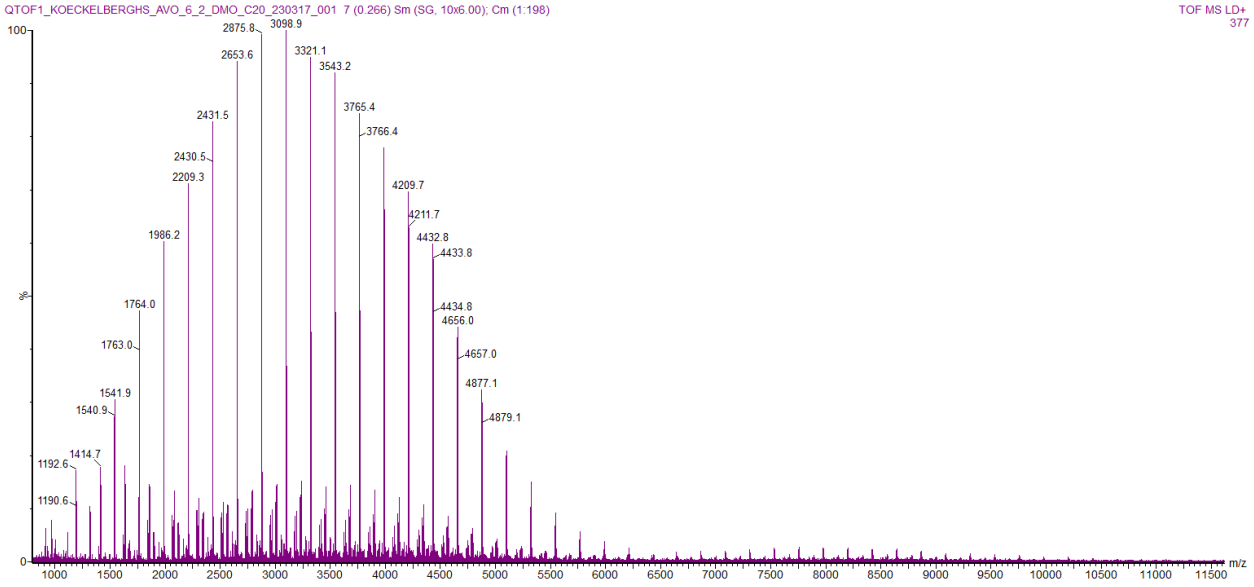

Figure S24. MALDI-ToF spectrum of **cat.-P3DMOT** (M_n of 3.0 kg/mol).

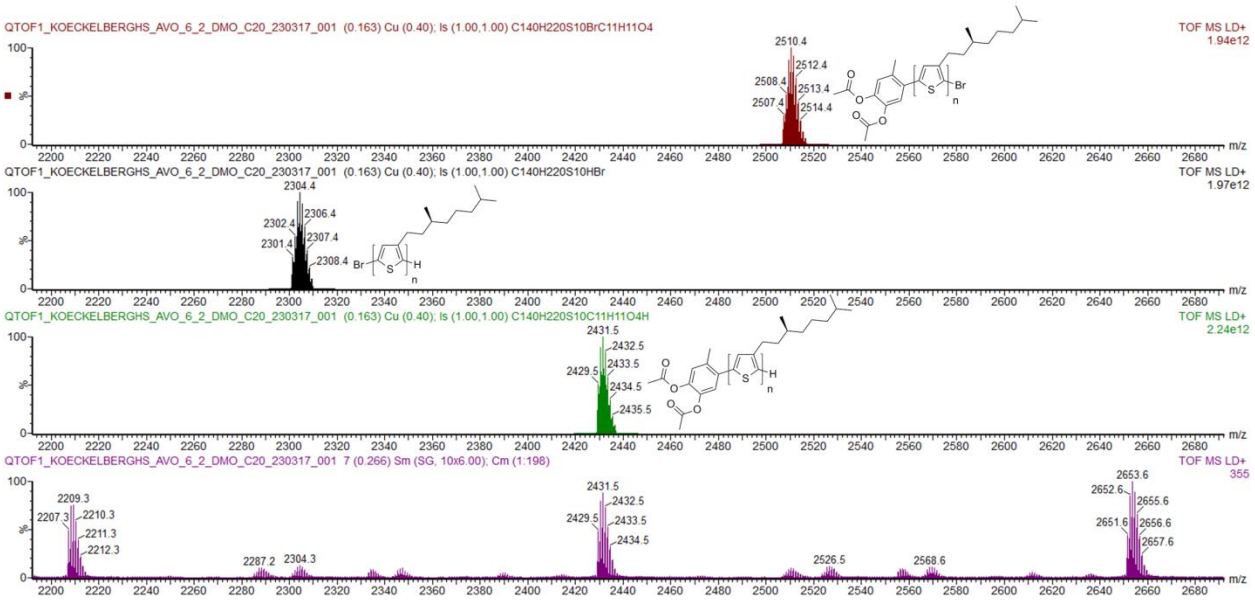

Figure S25. MALDI-ToF spectrum of **cat.-P3DMOT** (purple, M_n of 3.0 kg/mol) and predicted spectra for several possible end groups.

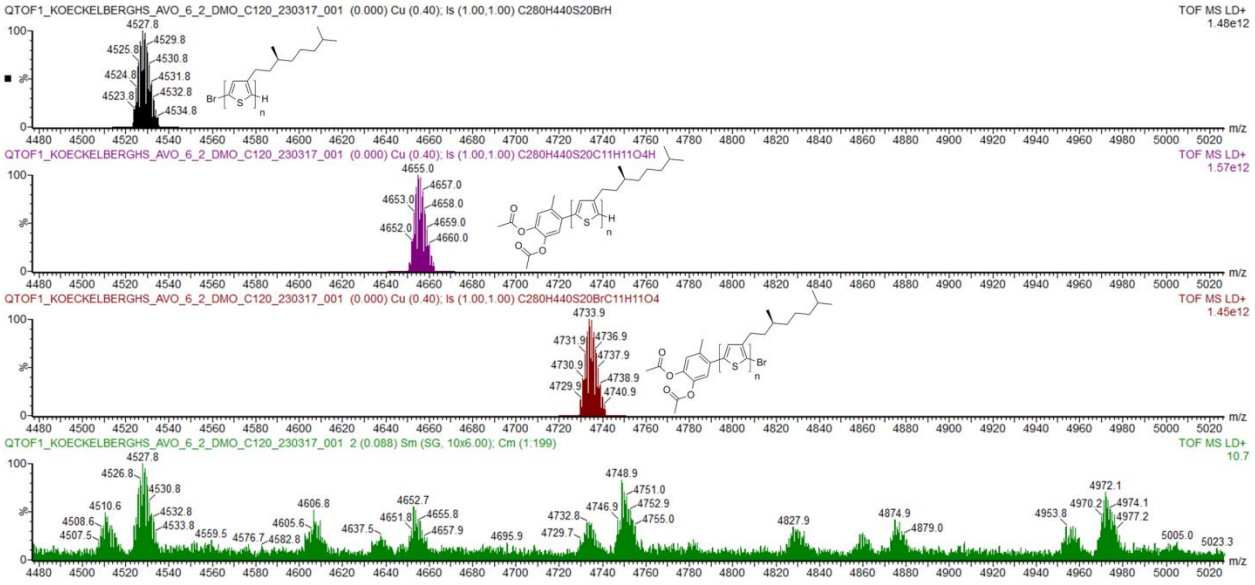

Figure S26. MALDI-ToF spectrum of **cat.-P3DMOT** (green, M_n of 15.5 kg/mol) and predicted spectra for several possible end groups.

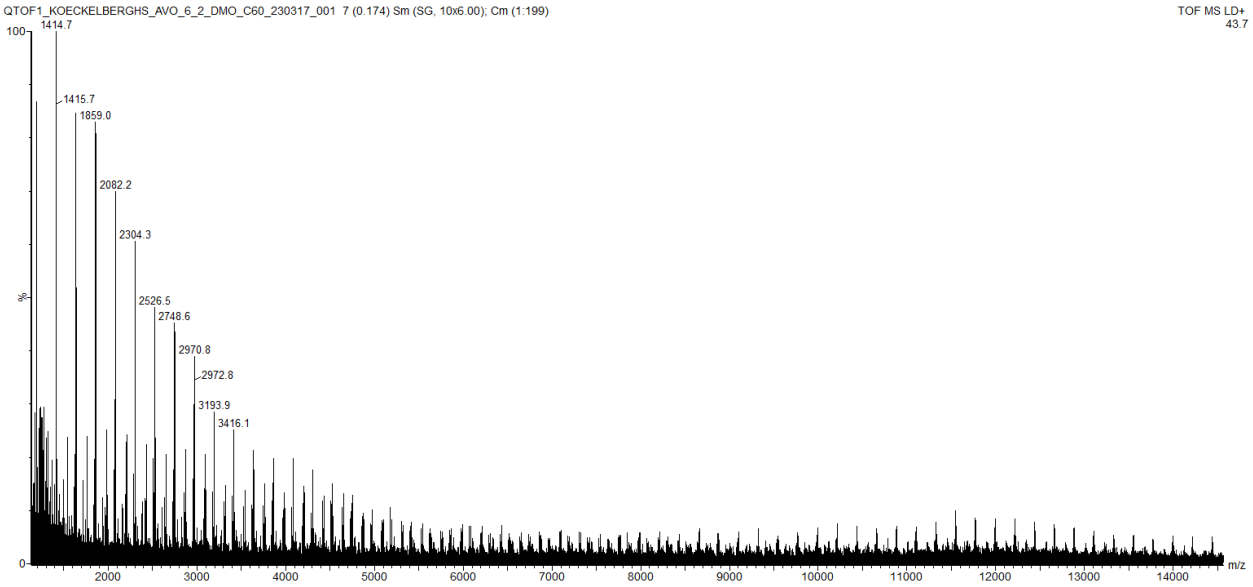

Figure S27. MALDI-ToF spectrum of **cat.-P3DMOT** (M_n of 10.2 kg/mol).

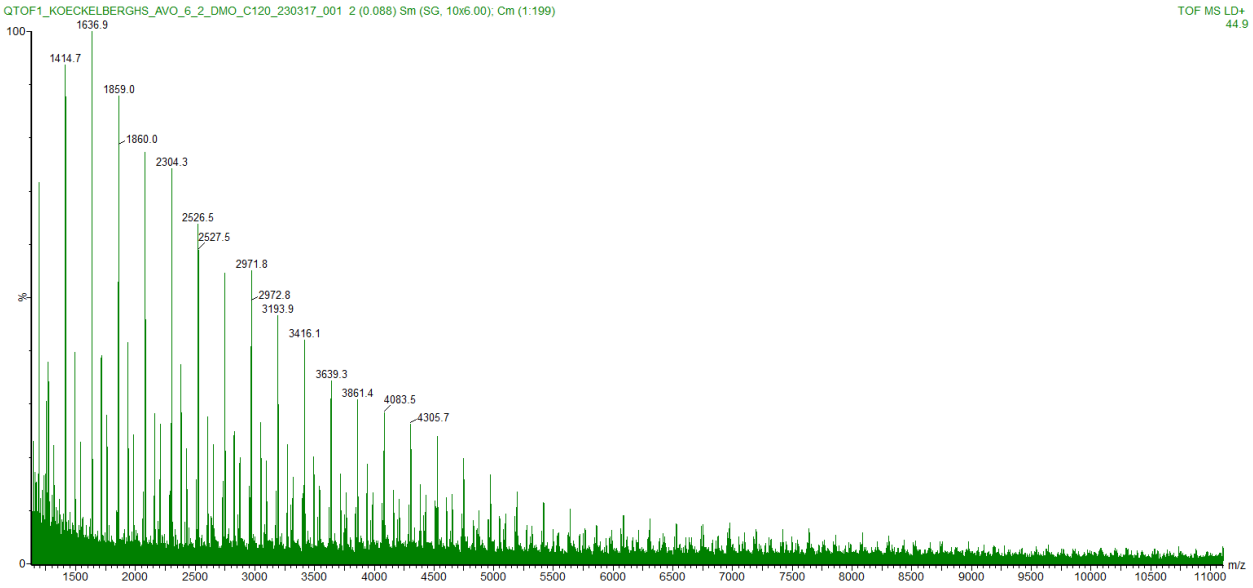

Figure S28. MALDI-ToF spectrum of **cat.-P3DMOT** (M_n of 15.5 kg/mol).

VI. Characterization of the hybrid material

a. AFM

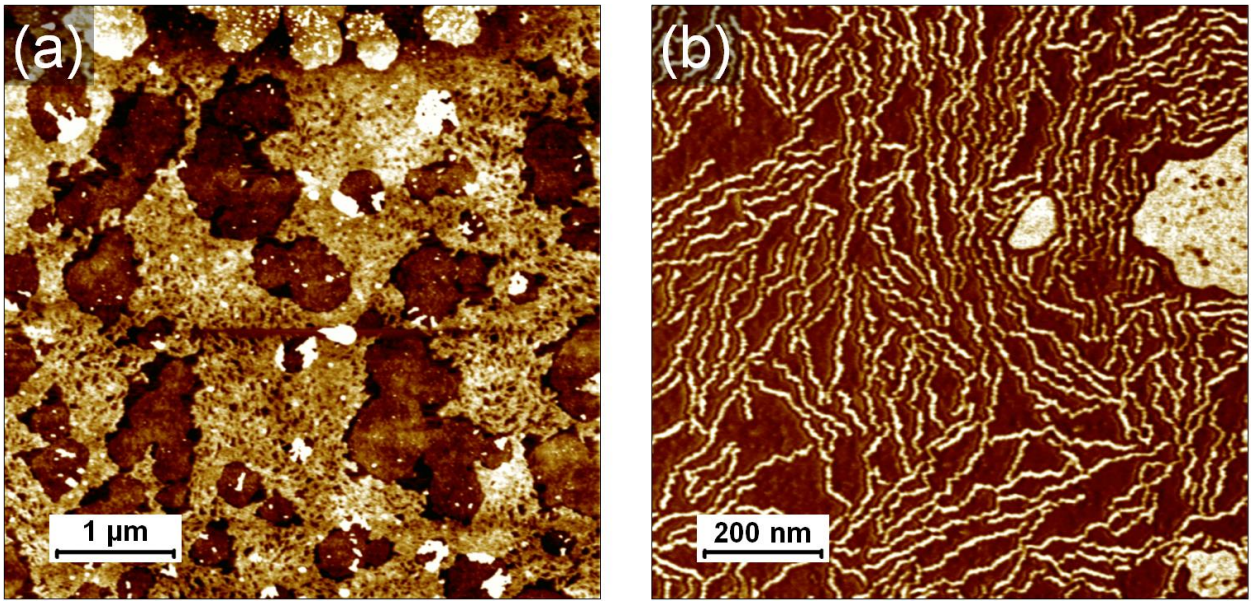

Figure S29. AFM topography (a) and phase (b) images of **cat.-P3DMOT** showing respectively the surface coverage by the polymers (brighter areas on the left image) and individually resolved fibers.

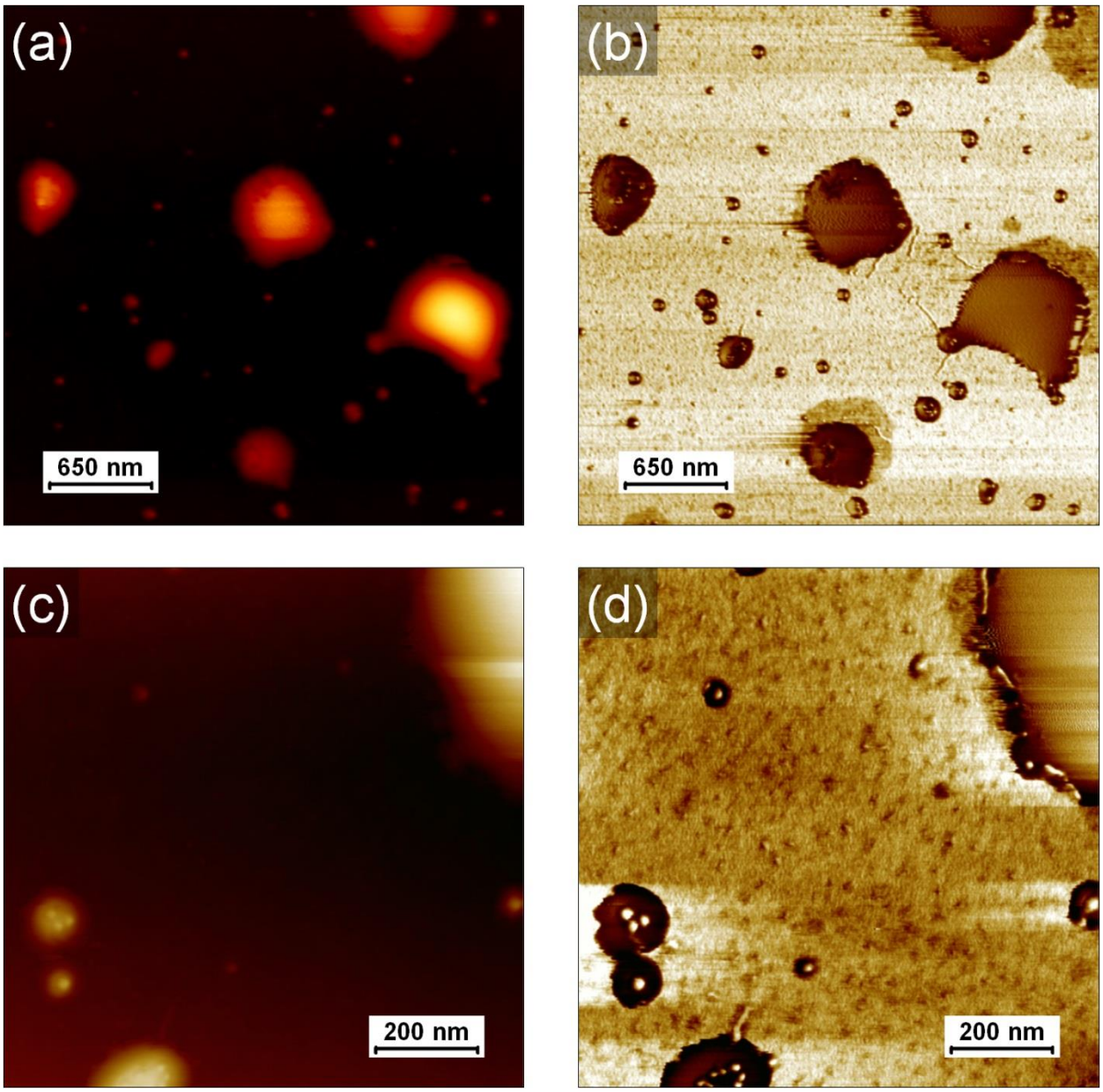

Figure S30. AFM topography (a, c) and phase (b, d) images of **Fe3O4-cat.-P3DMOT** showing that no fibers can be observed neither on the nanoparticles nor on the rest of the surface.

b. TEM

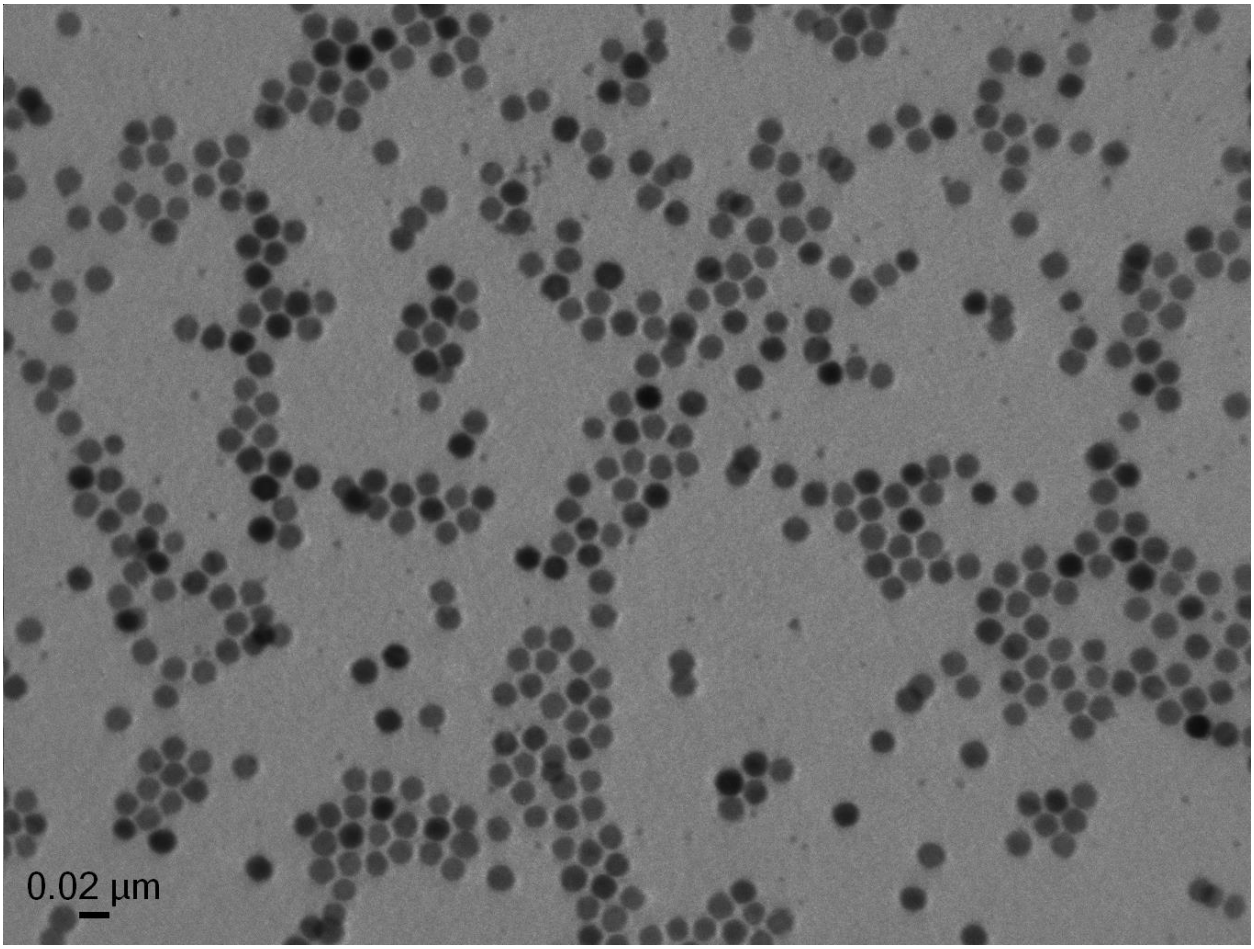

Figure S31. TEM measurement of the magnetite nanoparticles coated with oleic acid.

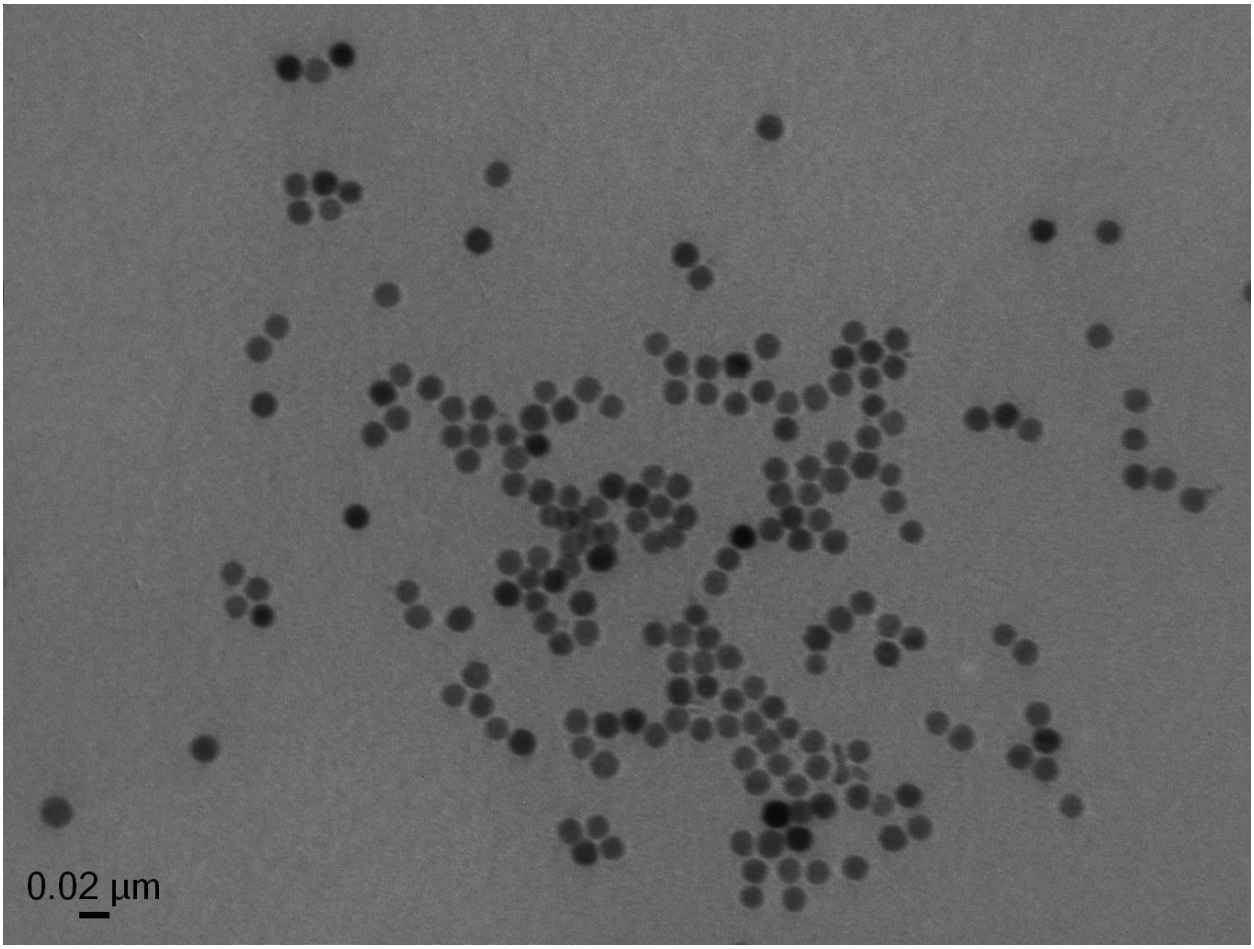

Figure S32. TEM measurement of **Fe_3O_4-cat.-P3DMOT**.

c. TGA

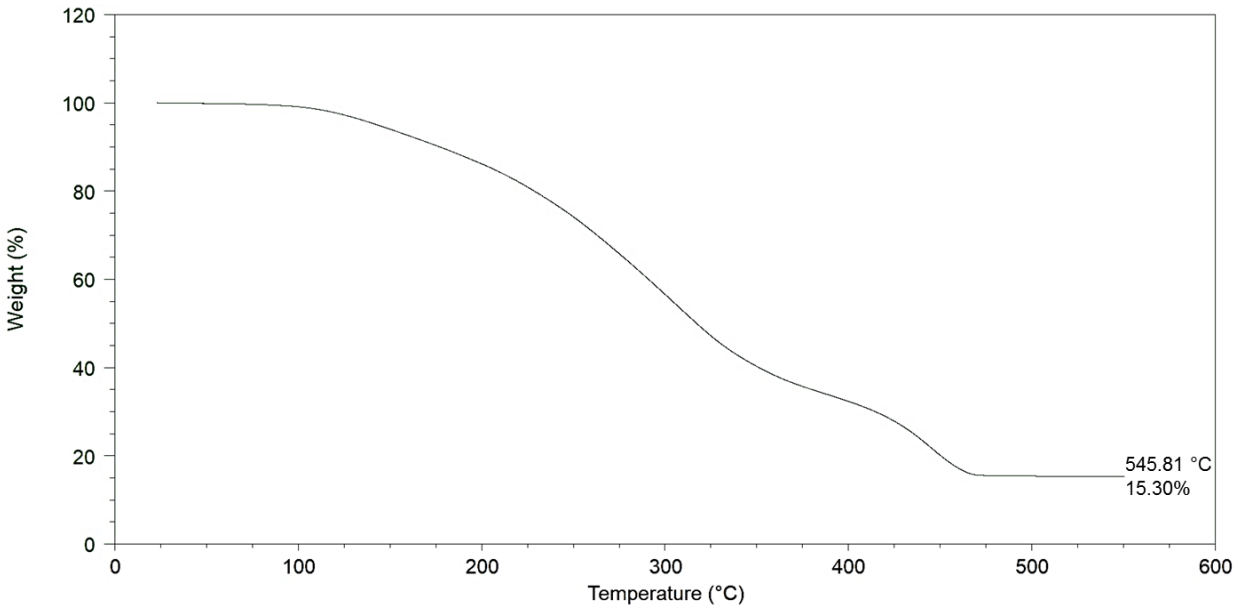

Figure S33. TGA measurement of **Fe_3O_4-cat.-P3DMOT**.

VII. References

1 I. Horcas, R. Fernández, J. M. Gómez-Rodríguez, J. Colchero, J. Gómez-Herrero and A. M. Baro, *Rev. Sci. Instrum.*, 2007, **78**, 13705.

2 S. Vandendriessche and T. Verbiest, eds. J. A. Shaw and D. A. LeMaster, 2013, vol. 8873, p. 88730Z.

3 A. Smeets, P. Willot, J. De Winter, P. Gerbaux, T. Verbiest and G. Koeckelberghs, *Macromolecules*, 2011, **44**, 6017–6025.

4 K. Van den Bergh, J. Huybrechts, T. Verbiest and G. Koeckelberghs, *Chemistry*, 2008, **14**, 9122–9125.

5 F. Monnaie, W. Brullot, T. Verbiest, J. De Winter, P. Gerbaux, A. Smeets and G. Koeckelberghs, *Macromolecules*, 2013, **46**, 8500–8508.